SCIENTIFIC REPORTS

OPEN

SUBJECT AREAS:
CATALYSIS
HOMOGENEOUS CATALYSIS
CHEMISTRY
ORGANOMETALLIC CHEMISTRY

Received
4 April 2013

Accepted
9 September 2013

Published
2 October 2013

Correspondence and requests for materials should be addressed to S.K.M. (swadhin.mandal@iiserkol.ac.in)

The Non-innocent Phenalenyl Unit: An Electronic Nest to Modulate the Catalytic Activity in Hydroamination Reaction

Arup Mukherjee, Tamal K. Sen, Pradip Kr Ghorai & Swadhin K. Mandal

Department of Chemical Sciences, Indian Institute of Science Education and Research-Kolkata, Mohanpur-741252, India.

The phenalenyl unit has played intriguing role in different fields of research spanning from chemistry, material chemistry to device physics acting as key electronic reservoir which has not only led to the best organic single component conductor but also created the spin memory device of next generation. Now we show the non-innocent behaviour of phenalenyl unit in modulating the catalytic behaviour in a homogeneous organic transformation. The present study establishes that the cationic state of phenalenyl unit can act as an organic Lewis acceptor unit to influence the catalytic outcome of intermolecular hydroamination reaction of carbodiimides. For the present study, we utilized organoaluminum complexes of phenalenyl ligands in which the phenalenyl unit maintains the closed shell electronic state. The DFT calculation reveals that the energy of LUMO of the catalyst is mainly controlled by phenalenyl ligands which in turn determines the outcome of the catalysis.

Non-innocent ligands (NILs)[1] have long attracted attention because of their unusual redox properties and their apparent, often deceptive, ability to stabilize metals in unusual oxidation states. The NILs have been employed not only for spectroscopic studies[2,3] but also in different chemical transformations[4,5]. It may be postulated that due to the presence of easily accessible frontier orbitals in the NILs as compared to those of typical ligands, they facilitate electronic transfer through an inverted bonding process[6]. These ligands are now emerging as synthetically useful and attractive scaffolds with broad and exciting perspectives[7]. Nevertheless, fully exploring the potential of these NILs in group–transfer chemistry, energy storage and conversion, biological applications still remains in its early stage and in particular the influence of NILs in a catalytic reaction has remained in its infancy[8,9]. Though the area is dominated by coordination chemists[10] and spectroscopists looking at influence of NIL in metals oxidation state, this concept is gradually entering into the area of catalysis[8]. In particular, in the field of organometallic chemistry, the NILs are emerging with ample opportunities in the realm of catalysis[5].

In this context, recently we introduced phenalenyl (PLY) unit as a potential ligand backbone to study their influence on the catalytic activity in ring opening polymerization (ROP) reactions[11]. Phenalenyl is a well-known odd alternant hydrocarbon with three fused benzene rings[12] with ability to form three redox species: cation, radical, and anion (Figure 1a) using its readily avaialable nonbonding orbital (NBO)[13]. The concept of designing neutral free radical based conductors using this nonbonding orbital of phenalenyl was first proposed by Haddon[14–17]. Subsequently, this idea led to the discovery of the best neutral organic conductor at room temperature[15]. Recent articles by Morita, Takui and Hicks described the present status of phenalenyl based material chemistry emphasizing the radical electronic state of phenalenyl molecule[12,18]. On the other hand, we posed a question whether the presence of the readily available nonbonding orbital in the cationic state of phenalenyl unit[19] (State 1, Figure 1a) can be utilized to design well-defined molecular catalysts which will influence the catalytic activity in a homogeneous organic transformation. It was postulated that on coordination to a metal ion, the phenalenyl unit will generate the closed shell cationic state and the empty NBO will function as electron acceptor. Recently, we have shown that the cationic state of phenalenyl unit when created with zinc metal coordination can be used as non-innocent building block for construction of spin memory device which functions based on the ability of electron acceptance of the phenalenyl unit[20].

In this study, we have chosen a homogeneous catalytic process, namely guanylation or hydroamination of carbodiimides with aromatic amines. Earlier study suggests that the hydroamination of carbodiimide proceeds via the methane liberation and formation of the metal-amide complex. The reaction proceeds via a transition state formed by interaction of amine and catalyst, presumably involving the transfer of electron density from amine to catalyst[21]. We became interested to study this particular homogeneous process to unravel the exact role of

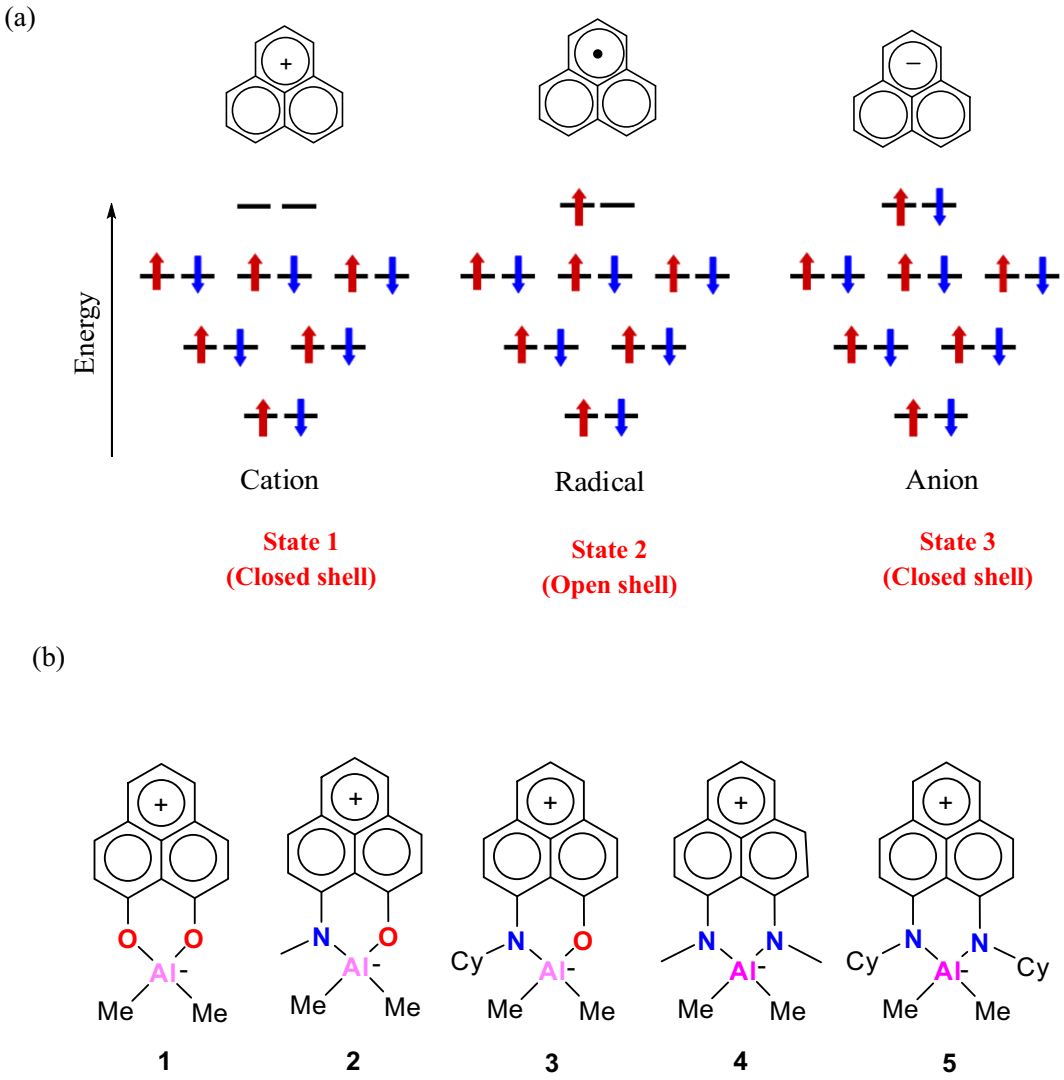

Figure 1 | (a) The three redox species of phenalenyl moiety: cation when the NBO is empty, radical when the NBO is singly occupied, and anion when the NBO is completely filled[19]; (b) Organoaluminum complexes **(1–5)** based on phenalenyl ligand.

non-innocent behavior of phenalenyl ligand in the catalytic outcome; since the influence of the NIL in catalytic reaction is not very well understood[8]. The catalytic addition of amine to carbodiimides (also known as guanylation or hydroamination) offers an efficient and atom-economical route to produce substituted guanidines, which is of great interest to academic and industrial researchers[22]. As a part of our ongoing interest in the development of catalytic systems for hydroamination reaction[23–25], herein we report the catalytic activity of a series of phenalenyl ligand based organoaluminum complexes towards hydroamination of carbodiimides. In the present study, five organoaluminum complexes, namely [(O,O–PLY)]$AlMe_2$ (**1**), [N(Me),O–PLY] $AlMe_2$ (**2**), [N(Cy),O–PLY]$AlMe_2$ (**3**), [N(Me),N(Me)–PLY]$AlMe_2$ (**4**), and [N(Cy),N(Cy)–PLY]$AlMe_2$ (**5**) (Figure 1b) were used for catalytic hydroamination of carbodiimides to primary aromatic amines.

Results

Syntheses and characterization. This study utilized organoaluminum complexes of phenalenyl ligands based on O,O– (HO,O–PLY), N,O– [HN(Me),O–PLY and HN(Cy),O–PLY)] and N,N– [HN(Me), N(Me)–PLY and HN(Cy),N(Cy)–PLY] donor combinations. The organoaluminum complexes **1**, **2**, and **4** were synthesized according to the literature procedure[11]. Synthesis of the new organoaluminum complexes, **3** and **5** were accomplished by reacting [HN(Cy),O–PLY] and [HN(Cy),N(Cy)–PLY] ligands, respectively with $AlMe_3$ under the evolution of methane (Figure 2). A solution of [HN(Cy),O–PLY] or [HN(Cy),N(Cy)–PLY] ligand in toluene was added drop-by-drop to the solution of $AlMe_3$ in toluene in a 1 : 1.2 stoichiometric ratio at −78°C and finally heated at 90°C or at 110°C for 6 h or 24 h to yield the complex **3** or **5** (Figure 2). Absence of any characteristic N–H resonance at δ 12.5 or 14.0 ppm in C_6D_6 as revealed by the ^1H NMR spectrum of the reaction mixture establishes almost quantitative conversion of the reactants into products in case of **3** and **5**. Both complexes **3** and **5** were characterized by ^1H NMR, ^{13}C NMR spectroscopy, elemental analysis and single crystal X-ray diffraction studies. ^1H NMR spectra of **3** and **5** in C_6D_6 exhibit a singlet at δ 0.01 and −0.10 ppm, respectively attributing to the proton resonance arising from the methyl group bound to the aluminum ion. The ^{13}C NMR spectra of **3** and **5** in C_6D_6 exhibit a singlet at δ −4.5 and −3.5 ppm, respectively assigned to the ^{13}C resonance arising from the methyl group bound to the aluminum ion. The structures of complexes **3** and **5** were determined unambiguously by single crystal X-ray diffraction technique (Figure 2). Suitable crystals of **3** and **5** were obtained from cold toluene solution at −20°C and 0°C, respectively. Complexes **3** and **5** were crystallized in the monoclinic and triclinic space group $C2/c$ and $P\bar{1}$, respectively with one molecule in the

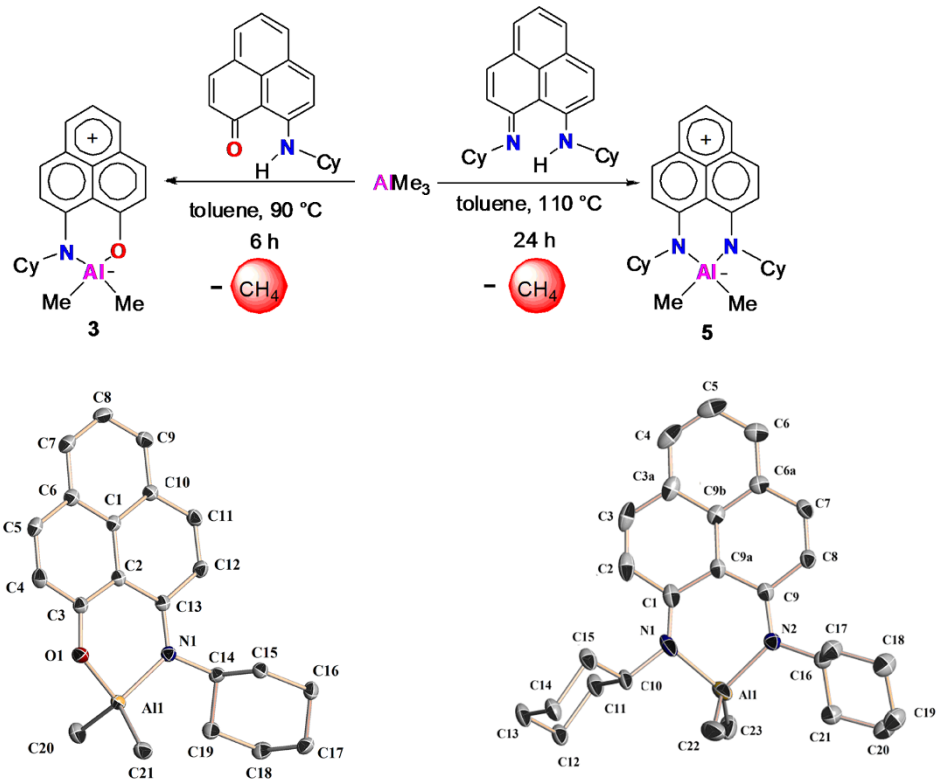

Figure 2 | Syntheses and molecular structures of the organoaluminum complexes 3 and 5 bearing phenalenyl ligands as determined by single crystal X-ray diffraction studies. Thermal ellipsoids are drawn with 50% probability level. Selected bond distances (Å) and angles (°) of (a) **3**: Al(1)–N(1) 1.9429 (15), Al(1)–O(1) 1.7820 (13), Al(1)–C(20) 1.9590 (19), Al(1)–C(21) 1.9659 (18), N(1)–C(13) 1.335 (2), O(1)–C(3) 1.3071 (19); N(1)–Al(1)–O(1) 95.19(6), N(1)–Al(1)–C(20) 112.02(7), O(1)–Al(1)–C(21) 107.30(7), C(20)–Al(1)–C(21)115.19(8); (b) **5**: Al(1)–N(1), 1.900(2)), Al(1)–N(2) 1.899(2), Al(1)–C(22), 1.981(3), AI(1)–C(23), 1.976(3), N(2)–AI(1) 1.896(9), N(1)–AI(1) 1.918(9), N(1)–Al(1)–N(2) 97.5(6), N(1)–Al(1)–C(27) 109.7(9), N(2)–Al(1)–C(26) 107.9(9), C(27)–Al(1)–C(26) 115.4(9).

asymmetric unit in both the cases. The X-ray structures of **3** and **5** reveal a distorted tetrahedral geometry around the aluminium ion. The observed Al–C bond distances in **3** are Al(1)–C(20), 1.9590 (19) Å and Al(1)–C(21) 1.9659(18) Å. Almost identical Al–C bond lengths are also observed in **5** [Al(1)–C(22), 1.981(3) Å; Al(1)–C(23), 1.976 (3) Å]. The Al–N (1.9429 (15) Å) bond distance found in **3** is longer than that observed in **2** (1.91 Å), while the Al–O bond distance (1.7820(13) Å) found in **3** is shorter than that observed in **2** (1.79 Å)[11]. The Al–N bond distances in **5** [Al(1)–N(1), 1.900(2) Å; Al(1)–N(2), 1.899(2) Å] are slightly shorter than that of the Al–N bond distances found in complex [(2,6–*i*Pr$_2$C$_6$H$_3$)NC(N*i*Pr$_2$)N(2,6–*i*Pr$_2$C$_6$H$_3$)]AlMe$_2$ (av. 1.9263 Å)[26].

Catalytic activity and the origin of non-innocence behaviour. Earlier, Bergman and co-workers[26] as well as Zhang and Xi[21] and co-workers have demonstrated that organoaluminum complexes can be used as a catalyst for the hydroamination/guanylation reaction of carbodiimides to produce substituted guanidines. These serve as building blocks for many biologically relevant compounds[27] and also used as suitable ligand system for stabilization of a wide range of metals[28]. Over the last decade, several catalytic systems have been developed based on main group metals[29–31], rare earth metals, and also by transition metals[32–37].

In the present study, the catalytic activity of the complexes **1**–**5** for hydroamination of carbodiimides with aromatic amines has been tested. The reaction of *p*-toluidine (CH$_3$–C$_6$H$_4$–NH$_2$, **6**) with *N*,*N*′-dicyclohexylcarbodiimide (CyN = C = NCy) was first examined under various conditions (Table 1). As a control experiment, CyN = C = NCy was mixed with *p*-toluidine in C$_6$D$_6$ at 25°C, but no reaction was observed even after 30 h (Table 1, entry 1). In contrast, addition of 5 mol% of **1** gave the desired *N*,*N*′,*N*″-trisubstituted guanidine (**7**) within 30 h at 25°C (Table 1, entry 2). Subsequently, the amount of catalyst loading was varied to see the most effective catalytic condition. It was found that 5 mol% of catalyst loading works at its best (Table 1, entries 2–4). Change of polarity of solvents showed influence on catalytic activity of **1** (Table 1, entries 2, 5, and 6). Increase of temperature from 25°C to 60°C showed significant enhancement in the reaction rate (Table 1, entries 2 and 7). Furthermore, the catalytic activity of **1** in different solvents (C$_6$D$_6$, THF-d$_8$, and CDCl$_3$) was tested by kinetic measurement through ^{1}H NMR spectroscopy to check the solvent effect on the catalytic reaction and the study reveals that C$_6$D$_6$ is the most effective solvent for the catalytic reaction (see Figure S2 of Supporting Information). Other organoaluminum complexes (**2**–**5**) were also found effective for this catalytic reaction under different reaction conditions (Table 1, entries 8–24). Complexes **2** and **3** displayed comparable catalytic activity only at higher temperature (80°C) leading to the formation of **7** in 97% and 95% yield, respectively (Table 1, entries 9 and 13). Similarly, complexes **4** and **5** exhibited the catalytic activity at 110°C producing **7** in 95% and 96% yield, respectively (Table 1, entries 18 and 22). This result clearly points out a distinct catalytic activity ordering, displaying the activity order **1** > **2** ~ **3** > **4** ~ **5** when the catalytic reactions were performed under identical condition.

In order to check the versatility of this catalytic process, we tested the catalytic activity of the complexes **1**–**5** with a series of aromatic amines and reacted with different carbodiimides (**8**–**17**) under the standardized catalytic condition (see Supplementary Information for details). The catalytic results reveal that complexes **1**–**5** are active catalysts for a wide range of substituted anilines having electron-donating as well as electron-withdrawing substituents (see

Table 1 | Standardization of reaction condition using *p*-toluidine and *N, N′*-dicyclohexyl carbodiimide as substrates[a]

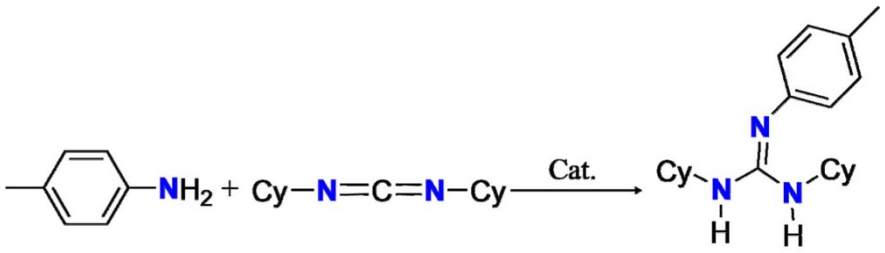

6 **7**

Entry	Cat. (mol%)	Solvent	Temp. (°C)	Time (h)	Yield (%)[b]
1	0	C_6D_6	25	30	–[c]
2	**1** (5)	C_6D_6	25	30	96
3	**1** (2.5)	C_6D_6	25	30	25
4	**1** (1)	C_6D_6	25	30	<5
5	**1** (5)	C_7D_8	25	36	88
6	**1** (5)	C_4D_8O	25	36	70
7	**1** (5)	C_6D_6	60	7.0	98
8	**2** (5)	C_6D_6	25	12	<5
9	**2** (5)	C_6D_6	80	7.0	97
10	**2** (2.5)	C_6D_6	80	7.0	35
11	**2** (1)	C_6D_6	80	7.0	15
12	**3** (5)	C_6D_6	25	12	<5
13	**3** (5)	C_6D_6	80	7.0	95
14	**3** (2.5)	C_6D_6	80	7.0	30
15	**3** (1)	C_6D_6	80	7.0	13
16	**4** (5)	C_6D_6	25	12	–[c]
17	**4** (5)	C_6D_6	80	12	<5
18	**4** (5)	C_6D_6	110	7.5	95
19	**4** (2.5)	C_6D_6	110	7.0	30
20	**4** (1)	C_6D_6	110	7.0	7.5
21	**5** (5)	C_6D_6	25	12	–[c]
22	**5** (5)	C_6D_6	110	7.5	96
23	**5** (2.5)	C_6D_6	110	7.0	26
24	**5** (1)	C_6D_6	110	7.0	5.0

[a]Conditions: *p*-toluidine, 0.2 mmol; *N,N′*-dicyclohexylcarbodiimide, 0.2 mmol.
[b]Yields were determined by ^{1}H NMR spectroscopy.
[c]No reaction.

Supplementary Information, Tables S1–S3). Complex **1** exhibited catalytic activity at 25°C and 60°C, while **2** and **3** exhibited comparable activity only at 80°C. Complexes **4** and **5** displayed the catalytic activity only at 110°C. Moreover, the catalytic table suggests that carbodiimides having different substituents are tolerable under the catalytic condition (see Supplementary Information, Tables S1–S3). The catalytic activity of these organoaluminum complexes were found to be moderate as compared to the earlier reported catalytic systems[22,26–30]. The detailed catalytic study carried out with complexes **1**–**5** clearly reveals that the catalytic activity of complex **1** (O,O-system) is highest and that of **4** and **5** (N,N-systems) are lowest, while the catalytic activity of complexes **2** and **3** (N, O-systems) falls in between the catalytic activity of O,O-donor based catalyst and N,N-donor based catalysts. In order to understand this difference in the catalytic activity between the organoaluminum complexes, we carried out a DFT calculation. Organoaluminum complexes of phenalenyl based ligands[11] as well as spirobiphenalenyl cationic boron systems[38] can be represented in different canonical forms in which most of the positive charge remains on the phenalenyl unit (see Figure S3 of the Supplementary Information). The nonbonding orbital of the cationic phenalenyl moiety remains empty in these dimethylaluminum complexes (**1**–**5**) which largely contributes to the LUMO of the molecule (also see Figure 1a). A DFT calculation at the 6–311 ++ G (d,p) level was carried out on organoaluminum complexes (**1**, **3**, and **5**) and the result reveals that in these complexes (**1**, **3**, and **5**), the LUMO predominantly resides over the phenalenyl part of the molecule (Figure 3a). Interestingly, the calculation reveals that the relative energy of the LUMO is largely determined by the nature of the phenalenyl ligands, in other words the phenalenyl ligands can tune the LUMO energy levels in these complexes. The energy of the LUMO (Figure 3b) gradually increases from **1** (−72.6 kcalmol^{-1}) to **3** (−63.3 kcalmol^{-1}) to **5** (−55.6 kcalmol^{-1}). This result points out that the existence of the lowest energy LUMO in **1** might lead to the best electron acceptance property of **1** among **1**, **3**, and **5** (Figure 3b). Additionally, the calculation reveals that the energy differences between LUMO and LUMO + 1 in these organoaluminum complexes are quite substantial. The energy differences between LUMO and LUMO + 1 are calculated as 45.1 kcalmol^{-1}, 42.0 kcalmol^{-1} and 39.5 kcalmol^{-1} in **1**, **3**, and **5**, respectively. Thus, the DFT calculation supports the presence of energetically accessible empty molecular orbital for electron acceptance in these phenalenyl-based organoaluminum complexes. In order to understand the electron acceptance property of these complexes, we carried out cyclic voltammetric study and these experiments indeed revealed the presence of two one-electron acceptance processes in case of **5** (Figure 4a), which can be explained by considering the generation of an anionic radical and a dianionic species (Figure 4b). The $E_{1/2}$ values ($E^1_{1/2}$ =

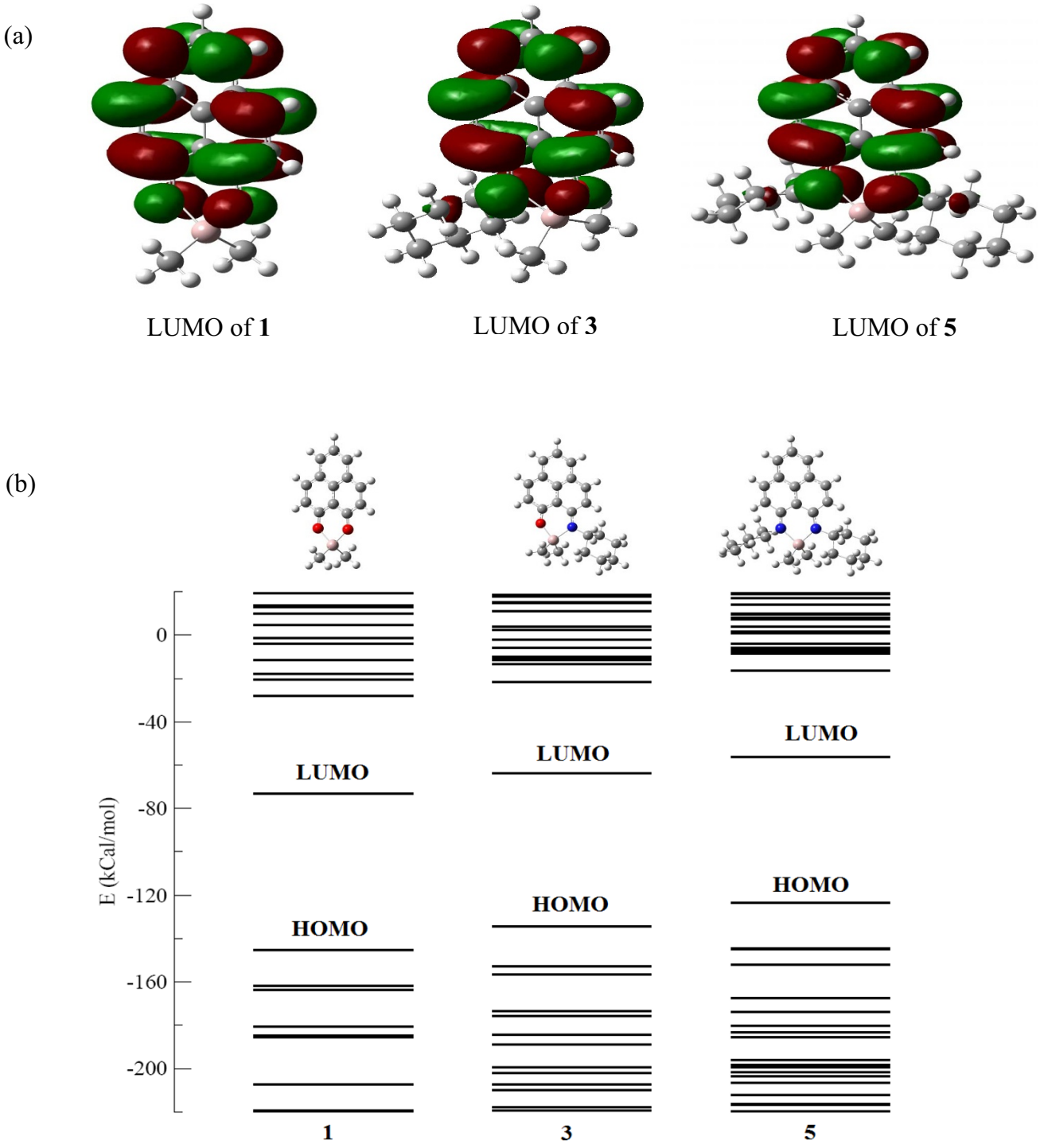

Figure 3 | (a) The computed LUMO of the complexes **1**, **3**, and **5**; (b) Molecular orbital energy profile diagram of the organoaluminum complexes (**1**, **3**, and **5**) showing that the nature of phenalenyl ligand can tune the energy of the LUMO in these complexes.

-1.49 V and $E^2_{1/2} = -1.80$ V) indicate that electron acceptance from the first to the second one becomes progressively difficult as a result of increasing Coulomb repulsion in the system. Early EPR studies on spirobiphenalenyl boron salt had shown[38] that the first reduction leads to the formation of an EPR active radical species and the second reduction results in the EPR silent anionic species supporting our result that the LUMO of a phenalenyl system can accommodate two electrons. Comparing the previous electrochemical data[11], it reveals that the reduction of **1** is much more facile and that of **4** or **5** is the most difficult among the series (the first half-wave reduction potential ($E^1_{1/2}$) values for **1**; $E^1_{1/2} = -0.87$ V, **2**; $E^1_{1/2} = -1.14$ V, **4**; $E^1_{1/2} = -1.45$ V, and **5**; $E^1_{1/2} = -1.49$ V, respectively). This result points out that the LUMO of **1** is most accessible for electron acceptance supporting our DFT calculation (see Figure 3b). However, this catalytic activity ordering may also have direct contribution from the Lewis accepting ability of the aluminum center as the attachment of more electronegative O,O-phenalenyl ligand (**1**) can make the aluminum center more Lewis acidic as compared to those with N,O-phenalenyl (**2** and **3**) and N,N-phenalenyl ligands (**4** and **5**). The charge calculation on aluminum center supports this fact as well which shows that the charge on aluminum is highest in catalyst **1** (1.80 a.u.), as compared to that in **3** (1.77 a.u.) and **5** (1.75 a.u.).

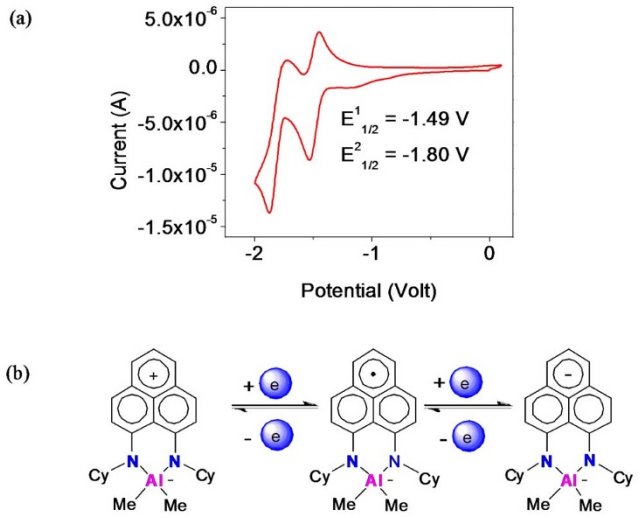

Figure 4 | (a) Cyclic voltammetry of **5** in acetonitrile, referenced to Ag/AgCl *via* internal ferrocene revealing two successive one electron reduction processes; (b) Successive electron acceptance by **5** generates an anionic radical and a di-anionic species.

Mechanistic study. The catalytic reaction was subjected to further study to gain more insight on the mechanistic process of the hydroamination reaction of carbodiimides and to correlate the catalytic results with the non-innocence behaviour of phenalenyl ligands. We adopted a combined approach using the kinetic studies, *in situ* NMR monitoring experiments, UV-vis absorption spectroscopy, Hammet study as well as DFT calculation. The study started with the detailed kinetic analysis to gather further insight into the hydroamination process of carbodiimide catalyzed by **1** using *p*-toluidine and *N*,*N*′-dicyclohexyl carbodiimide in C_6D_6. Kinetic studies for the formation of **7** were carried out with catalyst **1** and equi-molar amount of *p*-toluidine and *N*,*N*′-dicyclohexylcarbodiimide *via* ^{1}H NMR spectroscopy. The evolution of the specific resonances of the *N*,*N*′,*N*″-trisubstituted guanidine (**7**) was monitored by ^{1}H NMR spectroscopy relative to an internal standard (hexamethyl benzene) over the course of the first 7 h (see Figure S4 of Supporting Information for details). We first determined the order of the reaction with respect to amine concentration by keeping the concentration of other components virtually unaltered. Initially, we began our study with 21.71 mM of catalyst (**1**) concentration, and the carbodiimide to amine molar ratio was maintained at more than 10 : 1. A plot of concentration of amine against time followed an exponential decay of amine concentration (Figure 5a) which is consistent with the first-order kinetics. The first order rate of the reaction with respect to the amine concentration was further confirmed from the plot of $\ln(C/C_0)$ versus time, providing a linear plot with negative slope (Figure 5b)[39]. Next, we determined the order of the reaction with respect to the carbodiimide concentration by gradually varying concentration of carbodiimide. This study provided evidence of a first-order dependence of the reaction rate on carbodiimide concentration as well. The rate of reaction increases in a linear fashion with increasing concentration of carbodiimide (Figure 5c). The similar observation was noted by Marks and co-workers as well as by Hill and co-workers in case of intermolecular hydroamination reaction[39]. The individual rate constant values at different concentrations of carbodiimide were obtained after plotting $\ln(C/C_0)$ versus time. These plots provide a straight line with negative slope and from this first order plot, the individual rate constant values were obtained. The dependence of the reaction rate with respect to catalyst concentration was established by gradually changing the concentration of catalyst (from 7.5 mM to 15.1 mM) and holding the amine (151.6 mM) and carbodiimide (151.6 mM) concentrations fixed. A plot of reaction rate versus catalyst concentration reveals a linear increase of the reaction rate with increase of the catalyst concentration (Figure 5d). This observation suggests a first order dependence of the rate of the reaction with respect to the catalyst concentration. The first order rate of the reaction with respect to the catalyst concentration was further confirmed from van't Hoff plot[40]. A plot of $\ln k_{obs}$ versus ln[catalyst] provided a linear graph (Figure 5e) and the value of the slope was determined to be 1.42 (slope = order of the reaction)[40]. Related van't Hoff plot for intramolecular hydroalkoxylation mediated by lanthanide catalyst resulted in a slope of 1.43 as reported earlier[40], which compares well with the present observation.

Thus, from the present study, the overall rate law for the intermolecular hydroamination reaction of carbodiimides and amine catalyzed by **1** can be summarized as shown in eq. 1.

$$\text{rate} = k[\text{amine}]^1[\text{carbodiimide}]^1[\text{catalyst}]^1 \qquad (1)$$

Consequently, the kinetic study of the catalytic reaction suggests that the reaction rate depends on concentration of amine, carbodiimide, and catalyst. Subsequently, we carried out an *in situ* NMR study to understand the mechanistic aspect of the catalytic reaction in more details.

The *in situ* NMR study was recorded after mixing the organoaluminum complex **1** and *p*-toluidine in a 1 : 1 stoichiometric ratio and it revealed no detectable resonance of the CH_4 formation even after 5 h at 25 °C (Figure S7, Supporting Information). Earlier work by Zhang, Xi and co-workers have postulated the formation of aluminium-amide bond by activation of amine with concomitant elimination of methane[21]. Nevertheless, a close look on the ^{1}H NMR spectrum of 1 : 1 mixture of **1** and *p*-toluidine did indicate a shift in the aluminium bound methyl resonance as compared to that observed for pure catalyst. Furthermore, we observed that this shift is not specific to only 1 : 1 mixture of **1** and *p*-toluidine, rather it is common to the 1 : 1 stoichiometric reaction mixture of catalyst **2** or **4** and *p*-toluidine. Compound **1** exhibits the resonance of Al-Me group at δ 0.02 ppm, whereas in the 1 : 1 mixture of **1** and *p*-toluidine it shifts to more shielded region at δ −0.003 ppm (Figure 6a). However, this shift is smaller in case of the 1 : 1 mixture of **2** or **4** and *p*-toluidine (Figures 6b and 6c). This NMR shift indicates that the 1 : 1 mixture of catalyst and *p*-toluidine forms a donor acceptor adduct which is in equilibrium with the catalyst and *p*-toluidine. In this donor- acceptor interaction, the catalyst acts as an acceptor. The formation of such donor-acceptor aluminium amine adduct has been reported earlier by Wehmschulte and co-workers and others[41]. The larger NMR shift in case of 1 : 1 mixture of **1** and *p*-toluidine indicates stronger binding with **1** as compared to **2** or **4**. To further investigate this donor-acceptor interaction, we estimated association constant of this equilibrium process between the catalyst and *p*-toluidine by UV-vis absorption spectroscopic measurements of the reaction mixture of these organoaluminum complexes (**1**, **2**, and **4**) with *p*-toluidine (also see Supporting Information). Complex **1** shows the absorption maxima at λ 356, 426, and 451 nm, complex **2** shows the absorption maxima at λ 349, 445, and 471 nm, whilst **4** shows absorption maxima at λ 368, 501, and 541 nm. Next, the effect of the *p*-toluidine to the solution of the three complexes (**1**, **2**, and **4**) was checked in the UV-vis absorption spectra (Figure 6d–f) after a careful stepwise addition *p*-toluidine. Figure 6d suggests that with the increase of *p*-toluidine concentration, the absorptions of **1** at λ 356, 426, and 451 nm increases. Similar observation was also observed in case of **2** as well as **4** (Figure 6e and Figure 6f), although the change in absorption is less as compared to that observed with **1**. The association constant between the organoaluminum complexes and the *p*-toluidine was calculated from the UV-vis absorption spectroscopy using Benesi–Hildebrand equation (Figure 6g–i)[42,43]. A plot of $1/\Delta A$ (A = absorbance) versus 1/[amine] gives a straight line with positive slope in all the three cases (Figure 6g–i). The values of the association constants

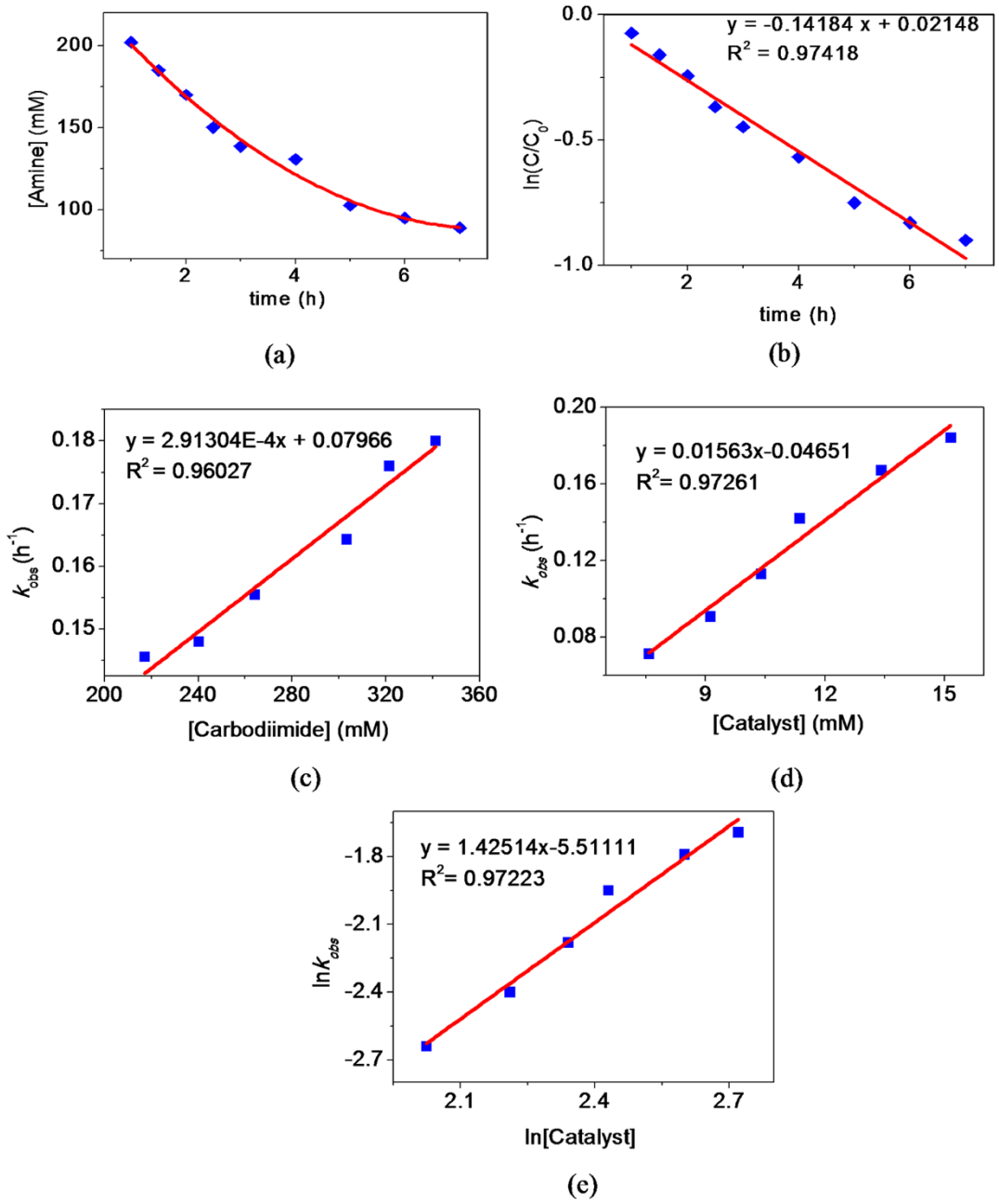

Figure 5 | Kinetic studies on the hydroamination of the carbodiimide for the formation of the guanidine (7) monitored by ^{1}H NMR spectroscopy in C_6D_6 at 25°C. (a) plot showing the change of amine concentration with time; (b) plot of ln(C/C$_0$) versus time; (c) plot of k_{obs} and concentration of carbodiimide for the formation of **7**; (d) plot of reaction rate versus concentration of catalyst and (e) van't Hoff plot for the formation of **7**.

calculated from these plots for **1**, **2**, and **4** are 7.02 × 10^4 M^{-1} (λ = 426 nm), 2.0 × 10^4 M^{-1} (λ = 445 nm), and 2.8 × 10^3 M^{-1} (λ = 541 nm), respectively (also see Supporting Information, Figure S9). These values suggest that the binding between complex **1** and *p*-toluidine is stronger than that with complexes **2** and **4**. The similar observation was also indicated from the ^{1}H NMR shift of Al-Me resonance of 1 : 1 catalyst-amine mixture. The binding affinities between these organoaluminum complexes and the amines may be attributed due to the lowest HOMO-LUMO energy gap between *p*-toluidine and **1** as compared to that calculated for **2** and **4** from the DFT study (Figure 7). Comparatively shorter HOMO-LUMO gap in case of **1** results in stronger donor-acceptor interaction. Furthermore, the addition of one equivalent carbodiimide into the 1 : 1 reaction mixture of **1** and *p*-toluidine triggered the formation of CH_4 at 25 °C as revealed by its characteristic resonance at δ 0.15 ppm[44] in ^{1}H NMR (Figure S8, see the Supporting Information). The resonance at δ 0.15 ppm becomes more prominent with the gradual progress of the reaction. This result points out that the presence of carbodiimide plays a crucial role in the methane evolution process and subsequent product formation. The formation of CH_4 on addition of one equivalent carbodiimide to the 1 : 1 stoichiometric reaction mixture of **1** and *p*-toluidine may be explained by considering that the carbodiimide shifts the initial equilibrium towards right and promotes the formation of aluminium-amide bond *via* methane evolution and amine activation process. Furthermore, in order to shed light on the cleavage of the amine N–H bond, we assessed the kinetic isotope effect. Determination of the kinetic isotope effect (KIE) has proven to be a very useful mechanistic tool, which has already been applied in organometallic systems[45]. The H/D kinetic isotope effect (KIE) measurement was performed using **6** and **6-d_2** in the presence of catalyst

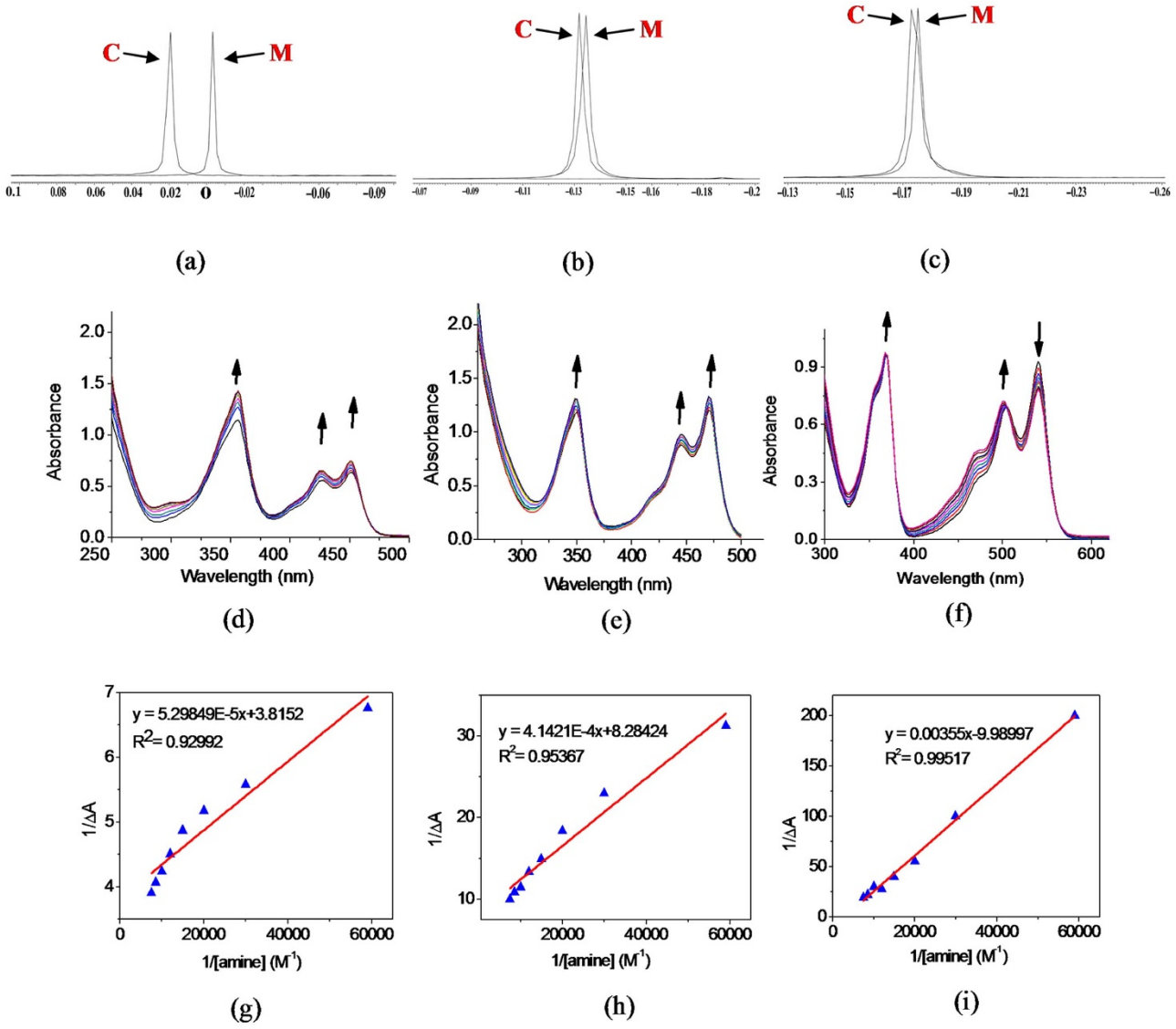

Figure 6 | The shift of Al-Me resonances in ^{1}H NMR spectra recorded in C_6D_6 (all ^{1}H NMR spectra are shown in identical scale). (a) 1 : 1 mixture of aluminium catalyst **1** and *p*-toluidine, (b) 1 : 1 mixture of aluminium catalyst **2** and *p*-toluidine, (c) 1 : 1 mixture of aluminium catalyst **4** and *p*-toluidine. Spectral key: C = pure catalyst **1** or **2** or **4** and M = 1 : 1 mixture of aluminium catalyst and *p*-toluidine. Electronic absorption spectra of (d) organoaluminum complex **1** with different concentration of *p*-toluidine in dichloromethane (e) organoaluminum complex **2** with different concentration of *p*-toluidine in dichloromethane; (f) organoaluminum complex **4** with different concentration of *p*-toluidine in dichloromethane. Benesi–Hildebrand plots (Plot of 1/ΔA (A = absorbance) vs.1/[amine]) for determination of binding constant of (g) *p*-toluidine with the complex **1** (λ = 426 nm) in dichloromethane; (h) *p*-toluidine with the complex **2** (λ = 445 nm) in dichloromethane and (i) *p*-toluidine with the complex **4** (λ = 501 nm) in dichloromethane.

1 in C_6D_6 under the identical reaction condition. The first order plots of the hydroamination of **6** and **6-d_2** under the reaction condition indicate k_{obs} = 0.07131 h^{-1} and k_{obs} = 0.02246 h^{-1}, respectively, which translates into a primary KIE of 3.17 (Figure 8). The KIE effect of 3.17 suggests that H/D derived from the $-NH_2/-ND_2$ moiety of **6**/**6-d_2** is involved in the slowest step (rate determining step) of the hydroamination of carbodiimides.

Discussion

Considering all these facts, the following mechanism was proposed for the organoaluminum complex catalyzed hydroamination of carbodiimide and primary aromatic amine. The dimethylaluminum complex **1** acts as a precatalyst and on addition of amine, it generates **18** which remains in an equilibrium with reactants. The equilibrium shifts to the forward direction after the addition of carbodiimide to the reaction mixture. This step is irreversible and occurs with elimination of methane gas leading to the formation of aluminium-amide bond by amine activation mechanism. The coordination of the nitrogen atom of the carbodiimide to aluminium ion facilitates the elimination of CH_4 and formation of intermediate **19**. This step is the rate determining step of the reaction as evidenced from the kinetic isotope effect study (*vide supra*). Additionally, the involvement of amine, carbodiimide and catalyst in the rate limiting step as proposed by this mechanism is also supported by our rate equation revealing the dependence of amine, carbodiimide and catalyst concentration (see eq. 1). Subsequently, the intermediate **19** rearranges via the insertion of carbodiimide into the Al-N bond and generates **20**. Earlier work by Zhang, Xi and co-workers have demonstrated such insertion of carbodiimide into the Al-N bond[21]. We eliminated another alternative ligand dissociation mechanistic pathway reported by Bergman and co-workers[26] since we did not observe any ligand dissociation during the catalytic cycle by NMR

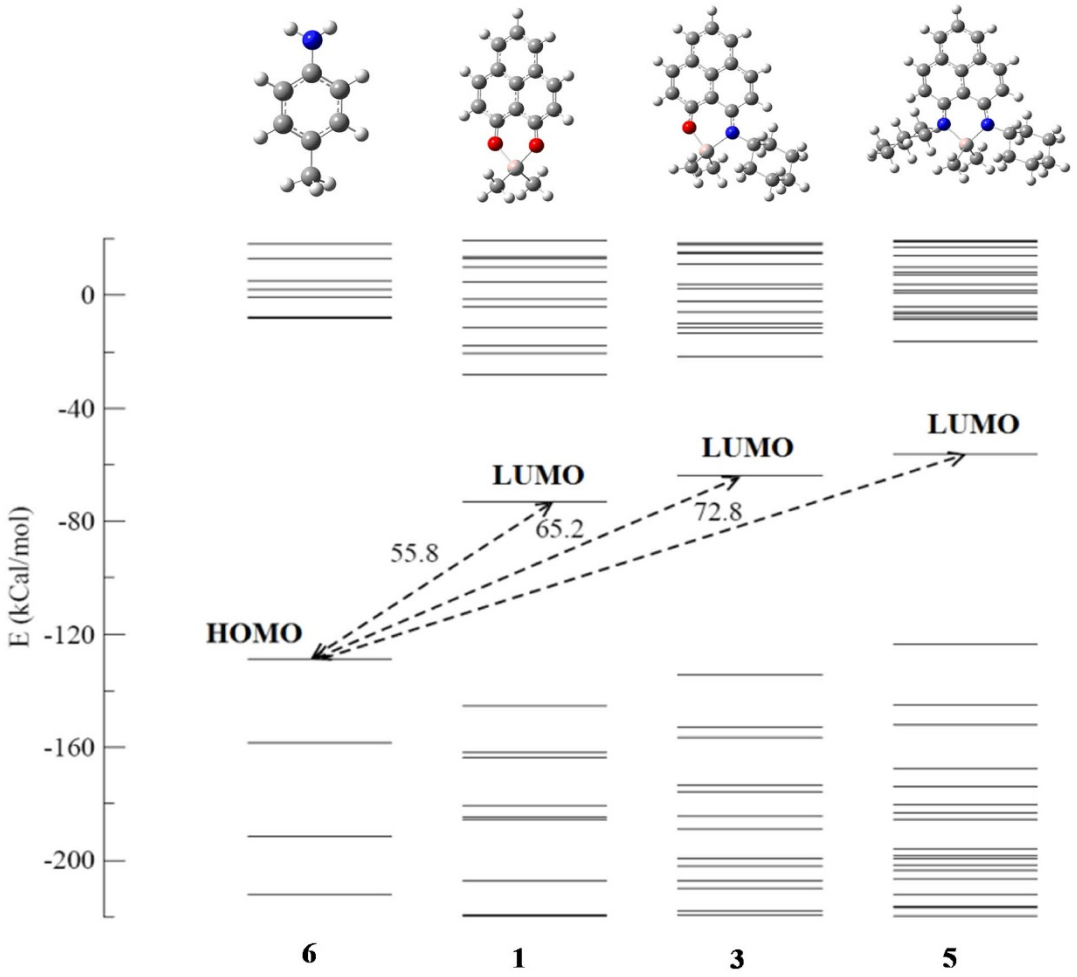

Figure 7 | **Molecular orbital energy profile diagram indicating that the HOMO–LUMO energy gap between aromatic amine (6) and catalyst is the lowest in case of 1.**

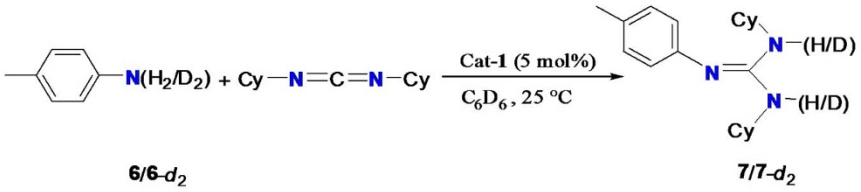

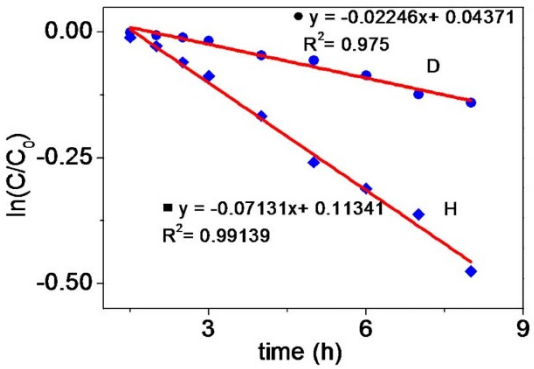

Figure 8 | **H/D KIE for the formation of 7 and 7-d_2 using catalyst 1 at 25°C.**

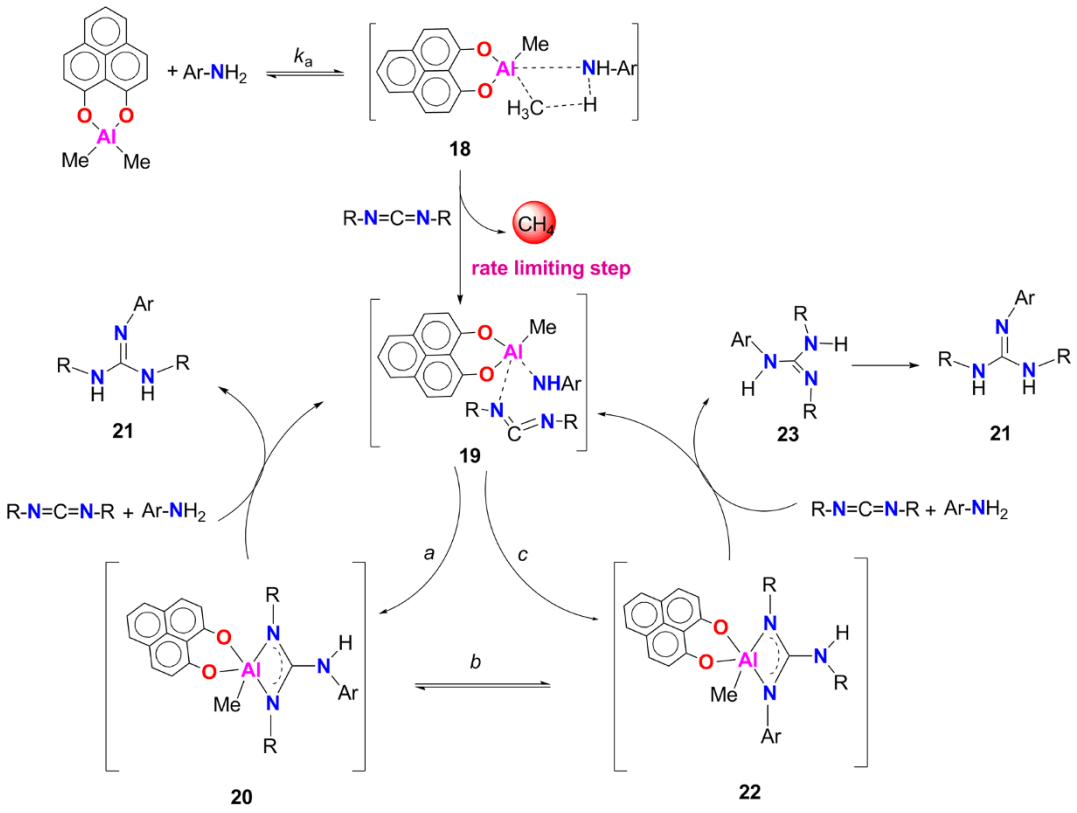

Figure 9 | Proposed mechanism for addition of primary aromatic amines to carbodiimides.

spectroscopy. Protonolysis of **20** by another molecule of primary amine and carbodiimide can regenerate **19** and can release the guanidine **21** (Figure 9) *via* path a. Also, there are two other pathways possible for aluminum catalyzed guanylation reaction as reported by Zhang, Xi and co-workers which cannot be ruled out. For example, intermediate **20** can rearrange into the guanidinate species **22** via path b through the intramolecular 1,3-hydrogen shift to form intermediate **22**. Protonolysis of **22** by another molecule of primary amine and carbodiimide can regenerate **19** and release the guanidine **21**. Moreover, intermediate **19** could also be rearranged to **22** directly to give the final desired product **21**, after protonolysis with primary amine and carbodiimide.

Furthermore, we have taken a closer look of the rate limiting methane elimination process with the help of DFT calculation which indicates that charge transfer takes place from the substrate to the phenalenyl part of the catalyst (see Figure S12, Supporting Information). Additionally, the Hammet study carried out to understand the effect of electron transfer. A Hammett plot of the resulting data provided a negative ρ value of -2.04 (Figure S13, Supporting Information). The negative ρ value supports that electron density is gained over the formation of transition state, a conclusion achieved by our DFT calculation on the transition state.

This study establishes that the cationic state of phenalenyl unit is not only useful for construction of the spin memory device by external spin injection[20] but also they can act as organic Lewis acceptor unit to influence the catalytic outcome of a homogeneous reaction. The non-innocent behaviour of a ligand in group-transfer chemistry, energy storage and conversion, biological applications is one of the most discussed topics in the contemporary literature. However, the influence of non-innocent behaviour of a ligand in catalytic processes has not been studied with full potential until now and this study is a step towards this direction. This study establishes that the cationic state of phenalenyl unit posing an energetically accessible LUMO can act as a Lewis acceptor organic unit which can influence the outcome of a catalytic reaction. The DFT calculation establishes that the energy of the LUMO of catalyst is mainly controlled by the phenalenyl ligand which in turn determines the activity of the catalyst for the catalytic process.

1. Jørgensen, K. Differences between the four halide ligands, and discussion remarks on trigonal-bipyramidal complexes, on oxidation states, and on diagonal elements of one electron energy. *Coord. Chem. Rev.* **1**, 164–178 (1966).
2. Jüstel, T. *et al.* Ruthenium complexes containing "noninnocent" *o*-benzoquinone diimine/*o*-phenylenediamide (2−) ligands. synthesis and crystal structure of the nitrido-bridged complex $[\{LRu(o\text{-}C_6H_4(NH)_2)\}_2(\mu\text{-}N)](PF_6)_2\cdot 3CH_3CN\cdot C_6H_5CH_3$. *Inorg. Chem.* **37**, 35–43 (1998).
3. Kaim, W., Wanner, M., Knödler, A. & Záliš, S. Copper complexes with non-innocent ligands: probing Cu^{II}/catecholato-Cu^{I}/*o*-semiquinonato redox isomer equilibria with EPR spectroscopy. *Inorg. Chim. Acta* **337**, 163–172 (2002).
4. Broderick, E. M. *et al.* Redox control of a ring-opening polymerization catalyst. *J. Am. Chem. Soc.* **133**, 9278–9281 (2011).
5. Chirik, P. J. & Wieghardt, K. Radical ligands confer nobility on base-metal catalysts. *Science* **327**, 794–795 (2010).
6. Szilagyi, S. K. *et al.* Description of the ground state wave functions of Ni dithiolenes using sulfur K-edge X-ray absorption spectroscopy. *J. Am. Chem. Soc.* **125**, 9158–9169 (2003).
7. Kaim, W. The shrinking world of innocent ligands: conventional and non-conventional redox-active ligands. *Eur. J. Inorg. Chem.* **2012**, 343–348 (2012).
8. Chirik, P. J. Forum on redox-active ligands. *Inorg. Chem.* **50**, 9737–9740 (2011).
9. Dzik, W. I., Vlugt, J. I. v. d., Reek, J. N. H. & d Bruin, B. Ligands that store and release electrons during catalysis. *Angew. Chem. Int. Ed.* **50**, 3356–3358 (2011).
10. Khusniyarov, M. M., Bill, E., Weyhermüller, T., Bothe, E. & Wieghardt, K. Hidden noninnocence: theoretical and experimental evidence for redox activity of a β-diketiminate (1-) ligand. *Angew. Chem. Int. Ed.* **50**, 1652–1655 (2011).
11. Sen, T. K. *et al.* Phenalenyl-based molecules: tuning the lowest unoccupied molecular orbital to design a catalyst. *Chem. Eur. J.* **18**, 54–58 (2012).
12. Morita, Y., Suzuki,S., Sato, K. & Takui, T. Synthetic organic spin chemistry for structurally well-defined open-shell graphene fragments. *Nature Chem.* **3**, 197–204 (2011).
13. Haddon, R. C. Design of organic metals and superconductors. *Nature* **256**, 394–396 (1975).

14. Mandal, S. K. *et al.* Resonating valence bond ground state in oxygen-functionalized phenalenyl-based neutral radical molecular conductors. *J. Am. Chem. Soc.* **128**, 1982–1994 (2006).
15. Pal, S. K. *et al.* Resonating valence-bond ground state in a phenalenyl-based neutral radical conductor. *Science* **309**, 281–284 (2005).
16. Mandal, S. K. *et al.* New family of aminophenalenyl-based neutral radical molecular conductors: synthesis, structure, and solid state properties. *J. Am. Chem. Soc.* **127**, 8185–8196 (2005).
17. Itkis, M. E., Chi, X., Cordes, A. W. & Haddon, R. C. Magneto-opto-electronic bistability in a phenalenyl-based neutral radical. *Science* **296**, 1443–1445 (2002).
18. Hicks, R. G. Switchable materials: a new spin on bistability. *Nature Chem.* **3**, 189–191 (2011).
19. Reid, D. H. The chemistry of the phenalenes. *Quart. Rev.* **19**, 274–302 (1965).
20. Raman, K. V. *et al.* Interface-engineered templates for molecular spin memory devices. *Nature* **493**, 509–513 (2013).
21. Zhang, W. X., Li, D., Wang, Z. & Xi, Z. Alkyl aluminum-catalyzed addition of amines to carbodiimides: a highly efficient route to substituted guanidines. *Organometallics* **28**, 882–887 (2009).
22. Zhang, W. X. & Hou, Z. Catalytic addition of alkyne C–H, amine N–H, and phosphine P–H bonds to carbodiimides: an efficient route to propiolamidines, guanidines, and phosphaguanidines. *Org. Biomol. Chem.* **6**, 1720–1730 (2008).
23. Mukherjee, A. *et al.* Assembling zirconium and calcium moieties through an oxygen center for an intramolecular hydroamination reaction: a single system for double activation. *Angew. Chem. Int. Ed.* **50**, 3968–3972 (2011).
24. Mukherjee, A. *et al.* Phenalenyl-based organozinc catalysts for intramolecular hydroamination reactions: a combined catalytic, kinetic, and mechanistic investigation of the catalytic cycle. *Chem. Eur. J.* **18**, 10530–10545 (2012).
25. Mukherjee, A., Sen, T. K., Mandal, S. K., Maity, B. & Koley, D. Construction of oxygen-bridged multimetallic assembly: dual catalysts for hydroamination reactions. *RSC Adv.* **3**, 1255–1264 (2013).
26. Koller, J. & Bergman, R. G. Highly efficient aluminum-catalyzed hydro-amination/-hydrazination of carbodiimides. *Organometallics* **29**, 5946–5952 (2010).
27. Berlinck, R. G. S. & Kossuga, M. H. Natural guanidine derivatives. *Nat. Prod. Rep.* **22**, 516–550 (2005).
28. Barker, J. & Kilner, M. The coordination chemistry of the amidine ligand. *Coord. Chem. Rev.* **133**, 219–300 (1994).
29. Alonso-Moreno, C. *et al.* Simple, versatile, and efficient catalysts for guanylation of amines. *Organometallics* **29**, 2789–2795 (2010).
30. Lachs, J. R. *et al.* Heavier group-2-element catalyzed hydroamination of carbodiimides. *Eur. J. Inorg. Chem.* **2008**, 4173–4179 (2008).
31. Ong, T.–G., O'Brien, J. S., Korobkov, I. & Richeson, D. S. Facile and atom-efficient amidolithium-catalyzed C−C and C−N formation for the construction of substituted guanidines and propiolamidines. *Organometallics* **25**, 4728–4730 (2006).
32. Zhu, X., Du, Z., Xu, F. & Shen, Q. Ytterbium triflate: a highly active catalyst for addition of amines to carbodiimides to *N*, *N′*, *N″*-trisubstituted guanidines. *J. Org. Chem.* **74**, 6347–6349 (2009).
33. Pi, C. *et al.* Multiple N−H bond activation: synthesis and reactivity of functionalized primary amido ytterbium complexes. *Organometallics* **26**, 1934–1946 (2007).
34. Pi, C., Zhu, Z., Weng, L., Chen, Z. & Zhou, X. Synthesis and structural characterization of lanthanide complexes with the di- or tri-anionic diguanidinate ligand: new insight into the flexibility and distinct reactivity of the linked diguanidinate ligand. *Chem. Commun.* **43**, 2190–2192 (2007).
35. Shen, H., Chan, H.-S. & Xie, Z. Synthesis, structure, and reactivity of $[\sigma:\eta^1:\eta^5\text{-}(OCH_2)(Me_2NCH_2)C_2B_9H_9]Ti(NR_2)$ (R = Me, Et). *Organometallics* **26**, 2694–2704 (2007).
36. Ong, T.-G., Yap, G. P. A. & Richeson, D. S. Catalytic C=N bond metathesis of carbodiimides by group 4 and 5 imido complexes supported by guanidinate ligands. *Chem. Commun.* **39**, 2612–2613 (2003).
37. Bazinet, P., Wood, D., Yap, G. P. A. & Richeson, D. S. Synthesis and structural investigation of *N*, *N′*, *N″*-trialkylguanidinato-supported zirconium(IV) complexes. *Inorg. Chem.* **42**, 6225–6229 (2003).
38. Chi, X. *et al.* The first phenalenyl-based neutral radical molecular conductor. *J. Am. Chem. Soc.* **121**, 10395–10402 (1999).
39. Brinkmann, C., Barrett, A. G. M., Hill, M. S. & Procopiou, P. A. Heavier alkaline earth catalysts for the intermolecular hydroamination of vinylarenes, dienes, and alkynes. *J. Am. Chem. Soc.* **134**, 2193−2207 (2012).
40. Seo, S. Y. & Marks, T. J. Lanthanide-catalyst-mediated tandem double intramolecular hydroalkoxylation/cyclization of dialkynyl dialcohols: scope and mechanism. *Chem. Eur. J.* **16**, 5148–5162 (2010).
41. Khandelwal, M. & Wehmschulte, R. J. Cationic organoaluminum compounds as intramolecular hydroamination catalysts. *J. Organomet. Chem.* **696**, 4179−4183 (2012).
42. Saha, S. *et al.* Specific recognition and sensing of CN^- in sodium cyanide solution. *Org. Lett.* **12**, 3406–3409 (2010).
43. Rosenthal, J. & Lippard, S. J. Direct detection of nitroxyl in aqueous solution using a tripodal copper(II) BODIPY complex. *J. Am. Chem. Soc.* **132**, 5536–5537 (2010).
44. Koller, J. & Bergman, R. G. Synthesis, characterization, and reactivity of aluminum alkyl/amide complexes supported by guanidinate and monoanionic OCO-pincer ligands. *Organometallics* **29**, 3350–3356 (2010).
45. Gómez-Gallego, M. & Sierra, M. A. Kinetic isotope effects in the study of organometallic reaction mechanisms. *Chem. Rev.* **111**, 4857–4963 (2011).

Acknowledgements

SKM thanks financial support from CSIR (Sanction Grant No. 01(2369)/10/EMR-II), New Delhi, India. Authors thank the anonymous reviewers for their valuable comments and suggestions to improve the manuscript. AM and TKS are thankful to IISER-Kolkata and CSIR, New Delhi respectively for respective research fellowships. PKG thanks DST, New Delhi, India for financial support. We gratefully acknowledge Prof. Dietmar Stalke and Markus Granitzka, Georg-August-Universität Göttingen for their X-ray structural help. We thank the NMR and X-ray facilities at IISER-Kolkata.

Author contributions

S.K.M. conceived the idea of this work and supervised the work to ascertain logical conclusions. A.M. carried out all catalysis reactions, kinetic studies, synthesis of organoaluminum complexes, data analysis. T.K.S. determined the X-ray structures of the organoaluminum complexes. P.K.G. carried out the DFT calculations. All the co-authors discussed and analysed the results. AM and SKM wrote the manuscript.

Additional information

Supplementary information accompanies this paper at http://www.nature.com/scientificreports

Competing financial interests: The authors declare no competing financial interests.

How to cite this article: Mukherjee, A., Sen, T.K., Ghorai, P.K. & Mandal, S.K. The Non-innocent Phenalenyl Unit: An Electronic Nest to Modulate the Catalytic Activity in Hydroamination Reaction. *Sci. Rep.* **3**, 2821; DOI:10.1038/srep02821 (2013).